

# Thermal Radiation from Solid Rocket Plumes at High Altitude

JOHN E. FONTENOT JR.\*  
The Boeing Company, New Orleans, La.

## Nomenclature

$A$	= cross-sectional area
$C_2$	= second Planck constant = $8.49 \times 10^{-2}$ ft-°R
$F$	= engine thrust
$I_{sp}$	= specific impulse
$L$	= effective thickness of particle cloud
$Q$	= radiant-heat rate
$T$	= temperature
$V$	= volume fraction of particles in plume
$W$	= weight fraction of particles in plume
$Z$	= $0.57 LVT/C_2$
$c$	= specific heat
$g_c$	= gravitational constant
$q$	= radiant-heat flux
$r$	= plume radius
$u$	= velocity
$u_{eff}$	= effective exhaust velocity
$\dot{w}$	= mass-flow rate
$x$	= axial distance from nozzle exit plane
$y$	= $(r - r_e)$
$\alpha$	= absorption coefficient
$\epsilon$	= emissivity
$\rho$	= density
$\sigma$	= Stefan-Boltzman constant
$\tau$	= mass per unit volume of plume
$\psi'''$	= tetragamma function

## Subscripts

$e$	= nozzle exit plane
$p$	= particle
$x$	= axial distance from nozzle exit plane
$t$	= total of gas and particle
$\lambda$	= wavelength

## Introduction

THE use of aluminized solid-propellant rockets on large boosters to provide for braking or ullage positioning during staging results in radiant heating of adjacent structure by the rocket exhaust. A method to predict heating from such an exhaust is necessary so that adequate heating protection can be provided where needed. Morizumi and Carpenter<sup>1</sup> have recently provided a rather sophisticated ap-

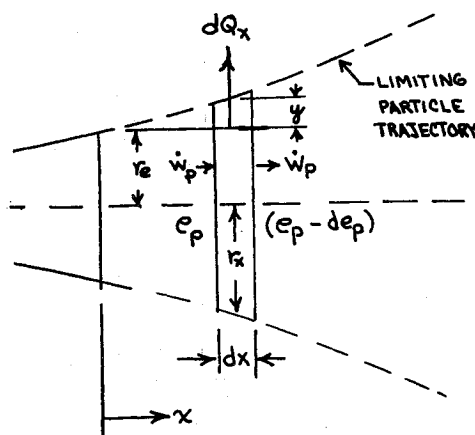


Fig. 1 Physical model.

proach to this problem. A simpler approach, providing easier estimation of heating rates, is presented here.

In an expansion from a nozzle into a near vacuum, the gas static temperature and density outside the nozzle are quite low. The result of the low gas density is a low gas emissivity, and the combination of low gas temperature and emissivity results in a negligible amount of gaseous radiation. For the exhaust of an aluminized solid rocket into a near vacuum, the total plume thermal radiation may be considered as that due to the cloud of metallic-oxide particles.

In an actual rocket plume, the particles vary in size over a considerable range, and their distribution and temperature through a cross section of the plume are not uniform. However, for purposes of this analysis, the particles will be assumed to be of a unique size and of a uniform distribution and temperature. This assumption is justified on the basis of material presented in the literature,<sup>1-3</sup> where a particle radius of  $2\mu$  is found to be a representative one. This will be the unique particle size assumed in this analysis.

## Analysis

Considering Fig. 1, the differential heat flux from the particle cloud can be written as

$$dQ_x = -\dot{w}_p c dT_{px} \quad (1)$$

The Stefan-Boltzman law gives

$$dq_x = \sigma \epsilon_{px} T_{px}^4 = dQ_x / 2\pi r_x [1 + (dr/dx)^2]^{1/2} dx \quad (2)$$

Combining Eqs. (1) and (2)

$$\frac{-dT_{px}}{T_{px}^4} = \frac{2\pi r_x \sigma \epsilon_{px} [1 + (dr/dx)^2]^{1/2} dx}{\dot{w}_p c}$$

Integrating this equation between the exit plane and any point  $x$  in the plume gives

$$\frac{1}{T_{px}^3} = \frac{1}{T_{pe}^3} + \frac{6\pi\sigma}{\dot{w}_p c} \int_0^x r_x \left[ 1 + \left( \frac{dr}{dx} \right)^2 \right]^{1/2} \epsilon_{px} dx \quad (3)$$

The plume radius at any point can be expressed as  $r_x = r_e + y(x)$ . Inserting this expression for  $r_x$  into Eq. (3) gives

$$\frac{1}{T_{px}^3} = \frac{1}{T_{pe}^3} + \frac{6\pi\sigma}{\dot{w}_p c} \int_0^x (r_e + y) \left[ 1 + \left( \frac{dy}{dx} \right)^2 \right]^{1/2} \epsilon_{px} dx \quad (4)$$

In Ref. 4, the monochromatic emissivity of a particle cloud is given as  $\epsilon_{\lambda p} = 1 - e^{-\alpha_{\lambda} V L}$ , where  $\alpha_{\lambda}$  is the monochromatic absorption coefficient of the particle cloud. McAdams<sup>4</sup> limits the application of this expression to semitransparent flames. Its application to particle clouds of optical thickness near one (the optical thickness of the exhaust plumes considered herein) needs to be justified. Sato and Matsumoto<sup>6</sup> used Eq. (4) to predict the emissivity of flames containing soot particles of  $2.87 \mu$  diam. The optical thicknesses of these flames ranged from 0.35 to 1.24. The good agreement between their theoretically predicted values and experimentally determined values justifies their use of Eq. (4). The agreement between the theoretical results obtained from use of this equation and experimental data, discussed herein, provides further justification.

An exact evaluation of  $\alpha_{\lambda}$  requires an expression dependent upon both the wavelength and temperature. To simplify the mathematics, it is assumed that the monochromatic absorption coefficient, in the temperature and frequency range of interest, can be written as  $\alpha_{\lambda} = 0.57/\lambda^{5.6}$ . The final justification for this assumption lies in the agreement between theoretical predictions and experimental results. With this assumption, the monochromatic emissivity can be written as  $\epsilon_{\lambda p} = 1 - e^{-0.57 V L \lambda}$ . To obtain the total particle emissivity, it is necessary to integrate over-all wavelengths. This integration yields<sup>5</sup>

$$\epsilon_{px} = 1 - (15/\pi^4) \psi'''(Z + 1) \quad (5)$$

Received August 5, 1964; revision received December 21, 1964.

\* Research Engineer, Launch Systems Branch, Aero-Space Division. Member AIAA.

where  $Z = 0.57 VLT_{pe}/C_2$ . The tetragamma function  $(15/\pi^4)\psi'''(Z+1)$  was evaluated using Ref. 7 and is plotted in Fig. 2 for  $Z = 0$  to 2. To evaluate  $Z$ , both  $V$  and  $L$  are needed. The volume fraction of particles in the cloud  $V$  is given by the ratio of mass of particles per unit volume of plume  $\tau_p$  to the density of the particle material  $\rho_p$ . But  $\tau_p$  is inversely proportional to the square of the plume radius  $r_e + y$ , thus

$$V = (\tau_{pe}/\rho_p)[r_e/(r_e + y)]^2 \quad (6)$$

If the view direction is normal to the plume axis, then

$$L = 2(r_e + y) \quad (7)$$

Substituting Eqs. (6) and (7) into the expression for  $Z$  gives

$$Z = 13.4 T_{pe}(\tau_{pe}/\rho_p)[r_e^2/(r_e + y)] \quad (8)$$

The particle mass per unit volume of the plume at the nozzle exit plane  $\tau_{pe}$  can be approximated from the performance characteristics of the rocket motor. Since

$$\tau_{pe} = W\tau_e = W(\dot{w}_t/A_e u_{eff})$$

and  $u_{eff} = g_c I_{sp}$  and  $\dot{w}_t = F/I_{sp}$ ,

$$\tau_{pe} = WF/g_c A_e I_{sp}^2 \quad (9)$$

Combining Eqs. (5), (8), and (9) and solving the resulting equation simultaneously with Eq. (4) will permit an evaluation of the particle cloud temperature and emissivity. Then from Eq. (2), the radiant-heat flux from the plume, as a function of  $x$ , can be evaluated, provided that  $\dot{w}_p$ ,  $c$ ,  $W$ ,  $F$ ,  $A_e$ ,  $I_{sp}$ ,  $\rho_p$ ,  $y$ , and  $T_{pe}$  are known. To determine the heat flux to any point, this value of  $dq_x$  can then be used with the appropriate shape factor.

The quantities  $W$ ,  $F$ ,  $A_e$ , and  $I_{sp}$  can be specified from the characteristics of the motor and propellant. If the particles are assumed solid, then  $c$  and  $\rho_p$  are known from the properties of the particle material, and  $\dot{w}_p$  can be evaluated from the expression  $\dot{w}_p = \tau_{pe} A_e u_{pe}$ . To obtain values of  $u_{pe}$ ,  $T_{pe}$ , and  $y$ , a two-phase supersonic-flow computer program is necessary, such as the one discussed in Ref. 8. Lacking a computer program of this type, approximations can be made for  $T_{pe}$  and  $u_{pe}$  from curves found in Ref. 9, if the combustion-chamber conditions are close to those for the nozzle studied in that reference. An approximation for  $y$  can be obtained by using particle trajectories presented in Ref. 1.

### Experimental Verification

The method outlined in the preceding section was used to determine the heat flux from the plumes of two rocket motors tested at a simulated high altitude.<sup>10,11</sup> The results of the analytical method are compared to the experimental data in Fig. 3. It can be seen that, in the case of the 37-in. rocket motor, agreement is quite good. For the HPC motor, the agreement near the nozzle exit is very good, but at a point 1 ft downstream serious disagreement exists.

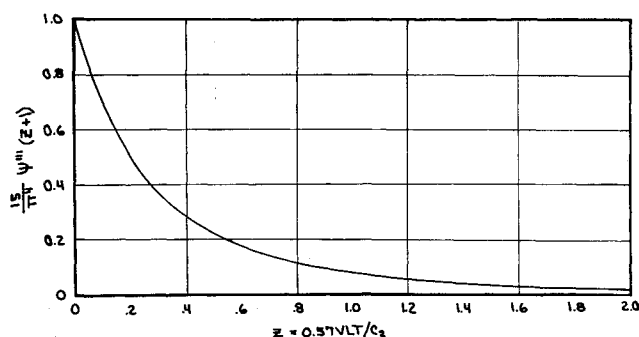


Fig. 2 Plot of the tetragamma function.

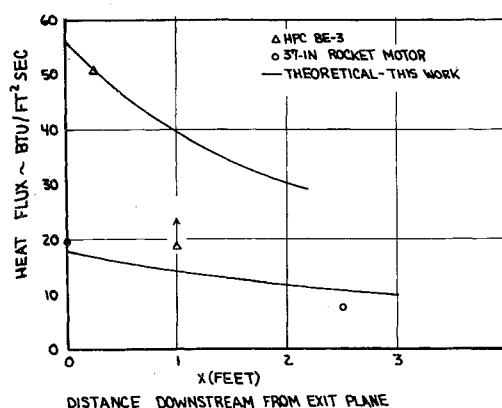


Fig. 3 Comparison of theoretical predictions with experimental data.

The nozzle exit conditions for the 37-in. rocket motor were determined by use of the computer program discussed in Ref. 8 and are thought to be known quite accurately. Since no computer calculations were available for the HPC motor, the nozzle exit conditions were approximated in the manner discussed previously. This, however, is not an explanation for the poor agreement between theory and experiment at the downstream location. The large decay in heat flux exhibited in the experimental data of Fig. 3 cannot be attributed solely to radiant heat transfer. Provided that the experimental data is accurate, the only plausible explanation for this phenomenon seems to be an unaccounted for chemical reaction.

### Discussion of Particle Emissivity

In the analysis of Ref. 1, the particle emissivity appeared as a parameter in the expression for cloud emissivity, whereas in Eq. 5 the value of particle emissivity does not enter. Morizumi and Carpenter found the particle emissivity, by indirect means, to be between 0.25 and 0.30. To determine the effective particle emissivity for the two rocket motors in question, the optical thicknesses of the particle clouds were calculated, and Fig. 4 of Ref. 1 was used to determine the particle emissivity. The particle cloud emissivity was calculated from Eq. 5. In both cases, the particle emissivity turned out to be 0.35, which, although slightly higher than Morizumi and Carpenter's value, agrees very well with the curves for aluminum oxide emissivity given by Morizumi and Carpenter.

A further comparison of the analysis of Ref. 1 with that presented here reveals that the particle cloud emissivity, as obtained in Ref. 1, is independent of particle temperature, whereas Eq. (5) and Fig. 2 indicate that  $\epsilon_p$  increases with particle temperature. Since Morizumi and Carpenter used a neutron scattering analogy to obtain cloud emissivity, the particle temperature did not enter, except through the dependence of the particle material emittance on temperature. However, in the analysis presented here, it enters quite naturally upon integration over all wavelengths. If a constant diameter plume with particle temperatures between 2000° and 5000°R is considered, Morizumi and Carpenter's approach predicts a constant value of emissivity, whereas Eq. (5) predicts a slowly decaying emissivity due to radiant heat transfer from the plume. The dependence or independence of cloud emissivity upon particle temperature has not been resolved experimentally at this time.

### References

- 1 Morizumi, S. J. and Carpenter, H. J., "Thermal radiation from the exhaust plume of an aluminized composite propellant rocket," AIAA Preprint 64-61 (January 1964).
- 2 Hoglund, R. F., "Recent advances in gas-particle nozzle flows," ARS J. 32, 662-671 (1962).

<sup>3</sup> Dobbins, R. A., "Measurement of mean particle size in a gas-particle flow," AIAA J. 1, 1940-1942 (1963).

<sup>4</sup> McAdams, W. H., *Heat Transmission* (McGraw-Hill Book Co., Inc., New York, 1954), 3rd ed., p. 100.

<sup>5</sup> Schack, A., "Radiation from luminous flames," Z. Tech. Physik 6, 530 (1925).

<sup>6</sup> Sato, T. and Matsumoto, R., "Radiant heat transfer from uminous flame," *International Developments in Heat Transfer* The American Society of Mechanical Engineers, New York, 1963), pp. 804-811.

<sup>7</sup> Davis, H. T., *Tables of the Higher Mathematical Functions*, Principia Press, Inc., Bloomington, Ind., 1935), Vol. II, pp. 34-69.

<sup>8</sup> Nickerson, G. R. and Kliegel, J. R., "The calculation of supersonic gas-particle flows in axis-symmetric nozzles by the method of characteristics," Space Technology Labs. Rept. 6120-3345-MU000 (May 1962).

<sup>9</sup> Bailey, W. S., Nilson, E. N., Serra, R. A., and Zupnik, T. F., "Gas particle flow in an axisymmetric nozzle," ARS J. 31, 793-798 (June 1961).

<sup>10</sup> Cimino, A. A. and White, D. W., "An investigation of rocket motor heat transfer to a surrounding spacecraft structure at simulated altitude conditions," Arnold Engineering Development Center, Arnold Air Force Station, Tenn., AEDC-TDR-63-79 (May 1963).

<sup>11</sup> Byrd, R. J., "Altitude base heating and ballistic performance tests of subscale second stage Minuteman wing VI motor," Arnold Engineering Development Center, Arnold Air Force Station, Tenn., AEDC-TDR-63-265 (January 1964).

## Numerical Solution of Magnetohydrodynamic Stagnation-Point Flow Equations

R. J. GRIBBEN\*

University of Southampton, Southampton, England

IN a problem on the magnetohydrodynamic, axisymmetric flow of a conducting fluid near a stagnation point recently considered by the writer,<sup>3</sup> similarity solutions of the Navier-Stokes and Maxwell equations are obtained from the solution of the ordinary differential equations

$$(F'''')/2 + (FF''/2) - \frac{1}{4}(F'^2 - 1) = \beta(H^2 - 1) \quad (1)$$

$$H'' + \epsilon FH' = 0 \quad (2)$$

satisfying  $F(0) = F'(0) = H(0) = 0$ ;  $F'(\infty) = H(\infty) = 1$ . The stream function and magnetic field are effectively  $F$  and  $H$ , and  $\beta$  and  $\epsilon$  are parameters defined in Ref. 3.

In the present note we describe a method of solving this coupled system of equations by successive approximations based on a method given by Weyl<sup>5</sup> for the nonmagnetic case. Weyl replaced the equation corresponding to (1) for  $F$  by an integral equation for  $F''$ , then approximated  $F''$  in the integrand. We extend this idea to include (2) and choose for the initial approximation an especially simple form for  $F$ . Recently, Davies<sup>1,2</sup> has applied a similar but rather more sophisticated process on a similar pair of equations.

Instead of (1) and (2) we consider the equivalent system,

$$F^{iv} + FF''' - 4\beta HH' \quad (3)$$

$$H'' + \epsilon FH' = 0 \quad (4)$$

satisfying

$$F(0) = F'(0) = H(0) = 0$$

$$F'''(0) = -\frac{1}{2} - 2\beta \quad F'(\infty) = H(\infty) = 1$$

For  $F$  known, (4) can be solved to yield

$$H(\zeta) = b \int_0^\zeta \exp \left[ -\epsilon \int_0^s F(t) dt \right] ds$$

where

$$\frac{1}{b} = \int_0^\infty \exp \left[ -\epsilon \int_0^s F(t) dt \right] ds$$

Following Weyl, we integrate (3) twice to produce the integral equation

$$\begin{aligned} G(\zeta) = & \left( \frac{1}{2} + 2\beta \right) \int_\zeta^\infty \exp \left[ -\int_0^s \frac{(s-t)^2 G(t) dt}{2} \right] ds - \\ & 4\beta b^2 \int_\zeta^\infty \exp \left[ -\int_0^s \frac{(s-t)^2 G(t) dt}{2} \right] \times \\ & \int_0^s \exp \left[ (1-\epsilon) \int_0^t \frac{(t-u)^2 G(u) du}{2} \right] \times \\ & \int_0^t \exp \left[ -\epsilon \int_0^u \frac{(u-v)^2 G(v) dv}{2} \right] dt ds \quad (5) \end{aligned}$$

for  $F''(\zeta) = G(\zeta)$ . The case  $\beta = 0$  gives the integral equation discussed by Weyl apart from a trivial modification in  $F$  and  $\zeta$ . For a given approximation  $G_n$ , (5) determines the next approximation  $G_{n+1}$ . However, here we choose to formulate the successive approximation scheme by means of the equations

$$F_{n+1}^{iv} + F_n F_{n+1}''' = 4\beta H_n H_n' \quad (6)$$

$$H_n'' + \epsilon F_n H_n' = 0 \quad (7)$$

satisfying

$$F_{n+1}(0) = F_{n+1}'(0) = H_n(0) = 0$$

$$F_{n+1}'''(0) = -\frac{1}{2} - 2\beta$$

$$F_{n+1}(\infty) = H_n(\infty) = 1$$

This is equivalent to the Weyl scheme but allows us to use, for our initial approximation, the function  $F_1 = c\zeta$ ,  $\zeta$  being the independent variable. Equation (7) then yields  $H_1$ , (6) yields  $F_2$ , and so on. The constant  $c$  is chosen so that all the boundary conditions are satisfied by  $H_1$  and  $F_2$ , and in addition  $F_2''(\infty) = 0$ . We find

$$H_1(\zeta) = (2\epsilon c)^{1/2} \int_0^\zeta \exp \left( \frac{-\epsilon c s^2}{2} \right) ds \left/ \left( -\frac{1}{2} \right) \right|$$

and, on integrating (6) three times (see Appendix),

$$\begin{aligned} F_2'(\zeta) = & \int_0^\zeta \int_\infty^v \exp \left( \frac{-cu^2}{2} \right) \left\{ \frac{8\beta \epsilon c}{[( -\frac{1}{2})!]^2} \times \right. \\ & \left. \int_0^u \exp \left[ \frac{(1-\epsilon)ct^2}{2} \right] \int_0^t \exp \left[ \frac{-\epsilon cs^2}{2} \right] ds dt - \right. \\ & \left. \left( \frac{1}{2} + 2\beta \right) \right\} du dv \quad (8) \end{aligned}$$

The boundary conditions  $H_1(0) = 0$ ,  $H_1(\infty) = 1$ ,  $F_2'''(0) = -\frac{1}{2} - 2\beta$ ,  $F_2''(\infty) = 0$ , and  $F_2'(0) = 0$  are all satisfied, and  $c$  is now determined by the equation  $F_2'(\infty) = 1$ , after which a further integration yields  $F_2(\zeta)$ , on applying the condition  $F_2(0) = 0$ . After integrating (8) by parts and some manipulation we find  $c = \frac{1}{2}$ . Note that  $c$  is independent of  $\beta$  and  $\epsilon$  so that  $H_1$  is known once and for all as an error function,  $H_1 = \text{erf}(\epsilon^{1/2}\zeta/2)/(\frac{1}{2})!$ , where

$$\text{erf} x = \int_0^x e^{-u^2} du$$

The writer had two exact solutions of (1) and (2), corresponding to  $\beta = 0$ ,  $H = 0$ , the well-known Homann solution (see, e.g., Ref. 4), and  $\beta = 1$ ,  $\epsilon = \frac{1}{16}$  (see Ref. 3). In